Clinical and Translational Oncology (2021) 23:296–310
https://doi.org/10.1007/s12094-020-02418-3

RESEARCH ARTICLE

The value of four imaging modalities to distinguish malignant from benign solitary pulmonary nodules: a study based on 73 cohorts incorporating 7956 individuals

Q. Wu[1] · L. Zhong[1,2] · X. Xie[1]

Received: 31 March 2020 / Accepted: 2 June 2020 / Published online: 16 June 2020

Abstract

Background Solitary pulmonary nodules (SPNs) frequently bother oncologists. The differentiation of malignant from benign nodules with non-invasive approach remains a tough challenge. This study was designed to assess the diagnostic accuracy of dynamic computed tomography (CT), dynamic magnetic resonance imaging (MRI), fluorine 18 fluorodeoxyglucose (^{18}F-FDG) positron emission tomography (PET), and technetium 99 m (^{99m}Tc) depreotide single photon emission computed tomography (SPECT) for SPNs.

Methods Electronic databases of MEDLINE, PubMed, EMBASE, and Cochrane Library were searched to identify relevant trials. The primary evaluation index of diagnostic accuracy was areas under the summary receiver-operating characteristic (SROC) curve. The results were analyzed utilizing Stata 12.0 statistical software.

Results Seventy-three trials incorporating 7956 individuals were recruited. Sensitivities, specificities, positive likelihood ratios, negative likelihood ratios, diagnostic score, diagnostic odds ratios, and areas under the SROC curve with 95% confidence intervals were, respectively, 0.92 (0.89–0.95), 0.64 (0.54–0.74), 2.60 (1.98–3.42), 0.12 (0.08–0.17), 3.10 (2.62–3.59), 22.24 (13.67–36.17), and 0.91 (0.88–0.93) for CT; 0.92 (0.86–0.95), 0.85 (0.77–0.90), 6.01 (3.90–9.24), 0.10 (0.06–0.17), 4.12 (3.41–4.82), 61.39 (30.41–123.93), and 0.94 (0.92–0.96) for MRI; 0.90 (0.86–0.93), 0.73 (0.65–0.79), 3.28 (2.56–4.20), 0.14 (0.10–0.19), 3.16 (2.69–3.64), 23.68 (14.74–38.05), and 0.90 (0.87–0.92) for ^{18}F-FDG PET; and 0.93 (0.88–0.96), 0.70 (0.56–0.81), 3.12 (2.03–4.81), 0.10 (0.06–0.17), 3.43 (2.63–4.22), 30.74 (13.84–68.27), and 0.93 (0.91–0.95) for ^{99m}Tc-depreotide SPECT.

Conclusion The dynamic MRI, dynamic CT, ^{18}F-FDG PET, and ^{99m}Tc-depreotide SPECT were favorable non-invasive approaches to distinguish malignant SPNs from benign. Moreover, from the viewpoint of cost-effectiveness and avoiding radiation, the dynamic MRI was recommendable for SPNs.

Keywords Solitary pulmonary nodules · CT · MRI · ^{18}F-FDG PET · ^{99m}Tc-depreotide SPECT

Introduction

Solitary pulmonary nodule (SPN), which is focal, circular, high density of solid lung shadow with diameter less than 3 cm, frequently initially emerges on chest radiography, or computed tomography (CT) images. Although there are about 20–30% of people having SPNs, 90% of them will not develop into malignancies. Hence, the oncologists are faced with the dilemma of choosing between biopsy of the SPNs and observation, and feel obliged to distinguish malignant nodules from benign with non-invasive approach. The optimal technique is to share the virtues of both early identifying malignancy and avoiding unnecessary surgery.

Electronic supplementary material The online version of this article (https://doi.org/10.1007/s12094-020-02418-3) contains supplementary material, which is available to authorized users.

✉ X. Xie
xiexianhe@fjmu.edu.cn

[1] Department of Oncology, The First Affiliated Hospital of Fujian Medical University, Chazhong Road No 20, Fuzhou 350005, Fujian, China

[2] Department of Medical Oncology, The Second Hospital of Longyan, Fujian 364000, China

Currently, the guidelines [1, 2] recommend using CT to evaluate SPNs. However, the problems of both radiation and low diagnostic specificity of CT for SPNs cannot be ignored. Additionally, it has been documented that the application of dynamic magnetic resonance imaging (MRI), fluorine 18 fluorodeoxyglucose (^{18}F-FDG) positron emission tomography (PET), and technetium 99 m (^{99m}Tc) depreotide single photon emission computed tomography (SPECT) to evaluate for diagnosis of SPNs in routine clinical practice recently. However, the standard non-invasive clinical strategy for SPNs remains to be established. Thereby, it is imperative to determine the diagnostic accuracy of the four imaging modalities in distinguishing malignant from benign SPNs based on the big data.

In 2008, Paul Cronin et al. had compared the application of dynamic CT, dynamic MRI, ^{18}F-FDG PET, and ^{99m}Tc-depreotide SPECT for SPNs [3]. However, it lacked of some crucial parameters, such as likelihood ratio (LR), diagnostic score, and diagnostic odds ratio (DOR). Moreover, during the ensuing decade, numerous articles about the four imaging modalities diagnosis of malignant SPNs sprung up. Therefore, we conducted this study based on a large scale (73 cohorts incorporating 7956 individuals) and more parameters to identify the competent approach to differentiate malignant SPNs from benign.

Materials and methods

Literature search

Researches were identified by a systematic electronic literature search for abstracts of relevant studies in the published literatures. MEDLINE, PubMed, EMBASE, and Cochrane Library were screened and updated to Nov 26, 2019. The following basic search terms were used: "computed tomography", "CT", "dynamic computed tomography", "dynamic CT", "dynamic contrast-enhanced computed tomography", "DCE CT", "magnetic resonance imaging", "MRI", "dynamic magnetic resonance imaging", "dynamic MRI", "dynamic contrast-enhanced magnetic resonance imaging", "DCE MRI", "positron emission tomography", "PET", "fluoro-2-deoxy-D-glucose positron emission tomography", "FDG PET", "single photon emission computed tomography", "SPECT", "^{99m}Tc-depreotide single photon emission computed tomography", "^{99m}Tc-depreotide SPECT", "solitary pulmonary nodule", "SPN", "solitary lung nodule", "diagnosis", "evaluation", "diagnostic test", "prediction". Full-text articles were reviewed if sufficient information were unavailable in abstracts. Moreover, the reference lists of related articles were scrutinized for additional studies. Reviews, case reports, letters to the editor, editorials comments, and conference abstracts were excluded. The search was carried out without any language restriction.

Selection of studies

Initially, two researchers, respectively, performed a screening of titles and abstracts, then scrutinized the full-text articles to hunt for relevant studies. Finally, we assessed eligibility and the methodologic quality of the trials, and summarized the diagnostic accuracy findings.

Inclusion criteria

Inclusion criteria were as following: (1) the parameters of dynamic CT, dynamic MRI, ^{18}F-FDG PET, and ^{99m}Tc-depreotide SPECT in evaluation of SPNs were available; (2) imaging results were compared with histologic sample (percutaneous or surgical biopsy or surgical resection) findings for more than half of the patients; (3) detailed raw data (i.e., true-positive, true-negative, false-positive, and false-negative findings) were available; (4) the sample size $\geq$ 10 patients.

Data extraction

Two investigators independently extracted data from all the recruited trials. All of the eligible studies contained the following information: the name of first author, continent of the research, year of publication, study design, and number of patients. Each investigator independently collected the data to analyze true-positive, true-negative, false-positive, and false-negative of imaging results.

Statistical analyses

Test performance metrics

Sensitivity, specificity, LRs, diagnostic score, and DOR with 95% confidence intervals (CIs) are recalculated from the contingency table of true-positive, true-negative, false-positive, and false-negative results.

Meta-analysis model

Parameters were calculated by using a bivariate mixed-effects regression model. The standard output of the bivariate model includes: mean logit sensitivity and specificity with their standard errors and 95% CIs; and estimation of the between-study variability in logit sensitivity and specificity and the covariance between them. Summary sensitivity, specificity, the corresponding positive likelihood ratios (PLRs), negative likelihood ratios (NLRs), diagnostic score, and DOR are derived as functions of the estimated model parameters. The

LRs indicate that by how much a given test would raise or lower the probability of having disease. The value of a DOR ranges from 0 to infinity, with higher values indicating better discriminatory test performance. The DOR is a single summary measure with the caveat that the same odds ratio may be acquired with different sensitivity and specificity. The area under the summary receiver-operating characteristic (SROC) curve serves as a global measure of test performance. The following guidelines used to interpret intermediate SROC values: low ($0.5 \leq AUC \leq 0.7$), moderate ($0.7 \leq AUC \leq 0.9$), and high ($0.9 \leq AUC \leq 1$) accuracy. In this study, all estimations were performed by using the MIDAS (bivariate mixed-effects regression model) module in Stata 12.0 software.

Assessment of quality and heterogeneity

Two reviewers independently assessed the quality of each study based on the prospectively developed criteria that were modified from well-accepted methodologic standards for evaluating quality in diagnostic test research; disagreements were resolved through discussion and consensus. The following nine criteria were evaluated, and a grade of 1 was given for each criterion that was fulfilled: prospective study design (prodesign), sample size of 30 or more subjects (ssize30), the uniform pathological biopsy reference standard test (fulverif), sufficient description of the reference standard (refdescr), adequate description of the validated test (testdescr), sufficient clinical description of subjects (subjdescr), adequate reporting of results (report), broad population (brdspect), and blinded interpretation of test results (blinded).

Heterogeneity among the studies is estimated graphically by Galbraith (radial) plot and statistically by I^2. A value of 0% indicates no observed heterogeneity, and values $\geq 50\%$ may be considered substantial heterogeneity. The advantage of I^2 is independent of the number of the studies in the meta-analysis.

Publication bias

Publication bias arises when the published studies only represent partial researches on a specific topic. It is assessed visually using a scatter plot, which is depicted as a symmetrical funnel shape when publication bias is absent [4], and $P < 0.05$ for the slope coefficient indicates significant asymmetry.

Results

Study identification

Initially, the search yielded 10,458 potential literature citations. Subsequently, 8572 were excluded for irrelevant, non-clinical trials, reviews, letters, case reports, and 1391 for duplicates. After verifying the related terms in the titles and abstracts, 392 irrelevant studies were removed, and 93 unfit designed studies were eliminated through analyzing the full text. Eventually, 73 published trials met inclusion criteria (see the supplemental data for details) (Fig. 1). There were 2 kinds of imaging modalities to assess the SPNs in 17 studies and 3 kinds of imaging modalities in 3 studies.

Study characteristics

The 73 studies incorporating 7956 patients were published ranging from 1990 to 2019. Among them, 49 trials were prospective; 25 trials were performed in America, 16 trials in Europe, and 28 trials in Asia. The average age of patients was 62.5, and the average number of nodules per study was 108. The final diagnosis for all subjects was confirmed pathologically in 37 studies while the final diagnosis was made either pathologically or clinically in 36 studies (Table 1).

Diagnostic parameters and summary assessment

For 31 dynamic CT studies, the pooled sensitivity was 0.92, 95% CI (0.89–0.95) (Fig. 2 CT1); the pooled specificity 0.64, 95% CI (0.54–0.74) (Fig. 2 CT1); the pooled PLR 2.6, 95% CI (2.0–3.4) (Fig. 2 CT2); the pooled NLR 0.12, 95% CI (0.08–0.17) (Fig. 2 CT2); the pooled diagnostic score 3.10, 95% CI (2.62–3.59) (Fig. 2 CT3); and the pooled DOR 22, 95% CI (14–36) (Fig. 2 CT3). The area under the SROC curve was 0.91, 95% CI (0.88–0.93) (Fig. 3a).

With regard to 14 dynamic MRI studies, the pooled sensitivity was 0.92, 95% CI (0.86–0.95) (Fig. 2 MR1); the pooled specificity 0.85, 95% CI (0.77–0.90) (Fig. 2 MR1); the pooled PLR 6.0, 95% CI (3.9–9.2) (Fig. 2 MR2); the pooled NLR 0.10, 95% CI (0.06–0.17) (Fig. 2 MR2); the pooled diagnostic score 4.12, 95% CI (3.41–4.82) (Fig. 2 MR3); and the pooled DOR 61, 95% CI (30–124) (Fig. 2 MR3). The area under the SROC curve was 0.94, 95% CI (0.92–0.96) (Fig. 3b).

Concerning 41 ^{18}F-FDG PET studies, the pooled sensitivity was 0.90, 95% CI (0.86–0.93) (Fig. 2 PET1); the pooled specificity 0.73, 95% CI (0.65–0.79) (Fig. 2 PET1); the pooled PLR 3.3, 95% CI (2.6–4.2) (Fig. 2 PET2); the pooled NLR 0.14, 95% CI (0.10–0.19) (Fig. 2 PET2); the pooled diagnostic score 3.16, 95% CI (2.69–3.64) (Fig. 2 PET3); and the pooled DOR 24, 95% CI (15–38) (Fig. 2 PET3). The area under the SROC curve was 0.90, 95% CI (0.87–0.92) (Fig. 3c).

Regarding 10 ^{99m}Tc-depreotide SPECT studies, the pooled sensitivity was 0.93, 95% CI (0.88–0.96) (Fig. 2 SPECT1); the pooled specificity 0.70, 95% CI (0.56–0.81) (Fig. 2 SPECT1); the pooled PLR 3.1, 95% CI (2.0–4.8) (Fig. 2 SPECT2); the pooled NLR 0.10, 95% CI (0.06–0.17)

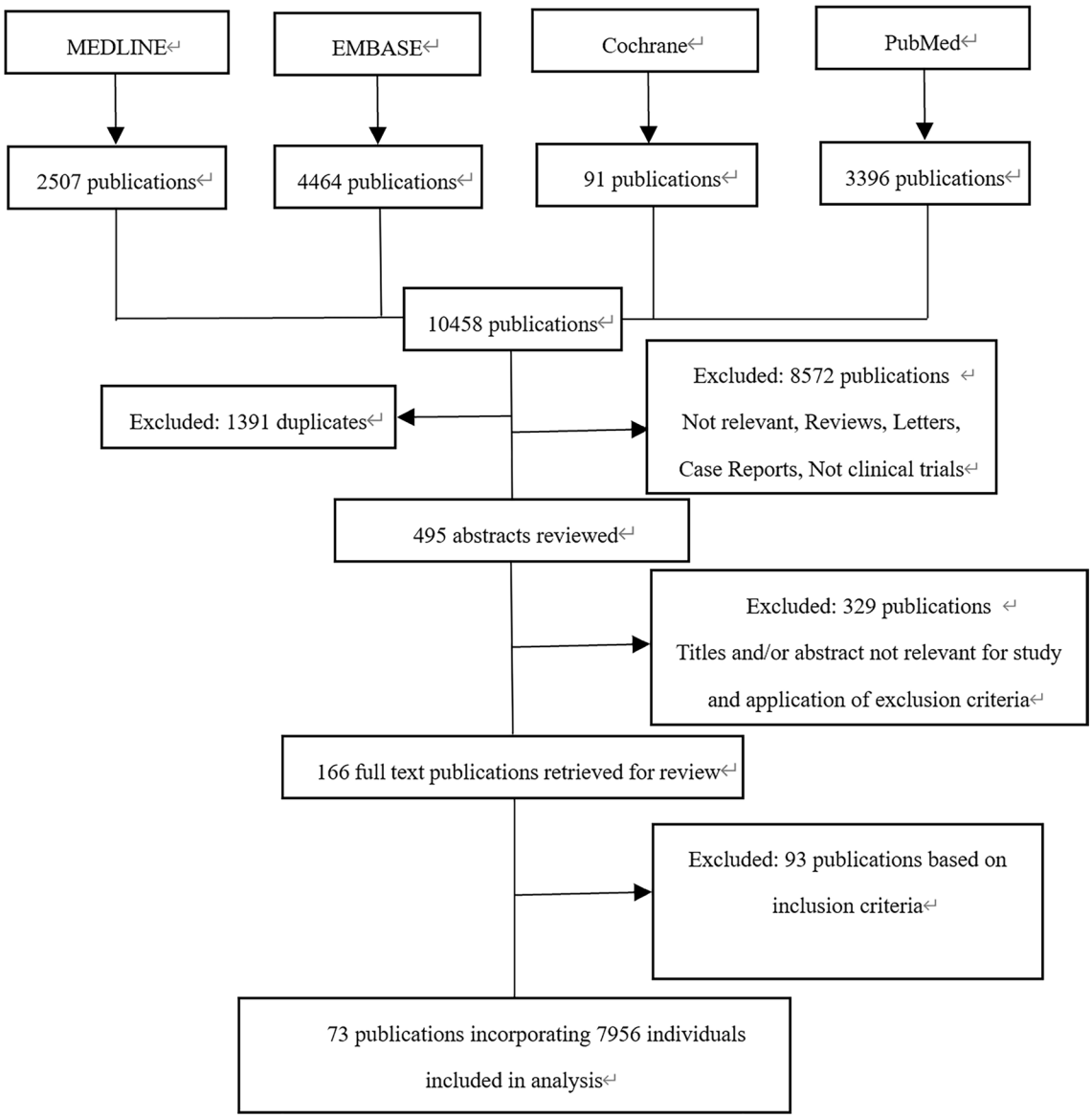

Fig. 1 Flow diagram of search strategies

(Fig. 2 SPECT2); the pooled diagnostic score 3.43, 95% CI (2.63–4.22) (Fig. 2 SPECT3); and the pooled DOR 31, 95% CI (14–68) (Fig. 2 SPECT3). The area under the SROC curve was 0.93, 95% CI (0.91–0.95) (Fig. 3d).

In summary, the four imaging modalities were promising in distinguishing malignant SPNs from benign, and the differences among them held no significance.

Study quality scores

The study quality scores of 31 dynamic CT trials (Fig. 4a), 14 dynamic MRI trials (Fig. 4b) and 10 ^{99m}Tc-depreotide SPECT trials (Fig. 4d) were ranged from 5 to 9 while that of 41 ^{18}F-FDG PET trials were 4 to 9 (Fig. 4c).

Study heterogeneity and publication bias

Concerning heterogeneity, the I^2 was 99% for dynamic CT (Fig. 5 CT1), 93% for dynamic MRI (Fig. 5 MR1), 99% for ^{18}F-FDG PET (Fig. 5 PET1), and 66% for ^{99m}Tc-depreotide SPECT (Fig. 5 SPECT1), respectively.

The analysis of meta-regression revealed that sources of heterogeneity for dynamic CT (Fig. 5 CT2), dynamic MRI (Fig. 5 MR2), ^{18}F-FDG PET (Fig. 5 PET2), and ^{99m}Tc-depreotide SPECT (Fig. 5 SPECT2) were shown in Fig. 5.

The *P* value of Deeks' Funnel Plot Asymmetry Test for dynamic CT (Fig. 5 CT3), dynamic MRI (Fig. 5 MR3), ^{18}F-FDG PET (Fig. 5 PET3), and ^{99m}Tc-depreotide SPECT (Fig. 5 SPECT3) were 0.65, 0.21, 0.74, and 0.61,

Table 1 Information of included studies

Author	Imaging modality	Year	Continent	Journal	Prodesign	Ssize30	Fulverif	Refdescr	Testdescr	Subjdescr	Report	Brdspect	Blinded
Ravinder K. Grewal [1]	Dynamic CT	2002	USA	Cancer J	Yes	Yes	No	Yes	Yes	Yes	Yes	No	No
Ravinder K. Grewal [1]	^{99m}Tc-depreotide SPECT	2002	USA	Cancer J	Yes	Yes	No	Yes	Yes	Yes	Yes	No	No
Blum J [2]	^{99m}Tc-depreotide SPECT	2000	USA	Chest	Yes	Yes	Yes	Yes	Yes	Yes	Yes	Yes	Yes
Arnaud Halley [3]	^{18}F-FDG PET	2005	Europe	Eur J Nucl Med Mol Imaging	Yes	No	No	Yes	Yes	Yes	Yes	Yes	No
Arnaud Halley [3]	^{99m}Tc-depreotide SPECT	2005	Europe	Eur J Nucl Med Mol Imaging	Yes	No	No	Yes	Yes	Yes	Yes	Yes	No
Gerarda J. Herder [4]	^{18}F-FDG PET	2004	Europe	Eur J Nucl Med Mol Imaging	No	Yes	No	Yes	Yes	Yes	Yes	Yes	No
Hiroaki Nomori [5]	^{18}F-FDG PET	2004	Asia	Ann Thorac Surg	Yes	Yes	Yes	Yes	Yes	Yes	Yes	Yes	Yes
Gang-Uei Hung [6]	^{18}F-FDG PET	2001	Asia	Jpn J Clin Oncol	Yes	No	Yes	Yes	Yes	Yes	Yes	Yes	Yes
Kotaro Higashi [7]	^{18}F-FDG PET	2001	Asia	J Nucl Med	Yes	Yes	Yes	Yes	Yes	Yes	Yes	Yes	Yes
Kotaro Higashi [7]	^{99m}Tc-depreotide SPECT	2001	Asia	J Nucl Med	Yes	Yes	Yes	Yes	Yes	Yes	Yes	Yes	Yes
Josephine Lee [8]	^{18}F-FDG PET	2001	USA	Chest	No	Yes	No	Yes	Yes	No	Yes	Yes	No
H. W. PRAUER [9]	Dynamic CT	1998	Europe	Br J Surg	Yes	Yes	Yes	Yes	Yes	Yes	Yes	Yes	Yes
H. W. PRAUER [9]	^{18}F-FDG PET	1998	Europe	Br J Surg	Yes	Yes	Yes	Yes	Yes	Yes	Yes	Yes	Yes
Val J. Lowe [10]	^{18}F-FDG PET	1998	USA	J Clin Oncol	Yes	Yes	Yes	Yes	Yes	Yes	Yes	Yes	Yes
Naresh Gupta [11]	^{18}F-FDG PET	1998	USA	Chest	Yes	No	Yes	Yes	Yes	No	Yes	Yes	Yes
Robert C. Hagberg [12]	^{18}F-FDG PET	1997	USA	Eur J Cardiothorac Surg	No	Yes	Yes	No	Yes	No	Yes	Yes	No
Naresh A. Dewan [13]	^{18}F-FDG PET	1997	USA	Chest	No	Yes	Yes	Yes	Yes	Yes	Yes	Yes	No
T. Bury [14]	^{18}F-FDG PET	1996	USA	Eur Respir J	Yes	Yes	Yes	Yes	Yes	Yes	Yes	Yes	No
Naresh C. Gupta [15]	^{18}F-FDG PET	1996	USA	J Nucl Med	Yes	Yes	Yes	Yes	Yes	Yes	Yes	Yes	Yes
Francis G. Duhaylongsod [16]	^{18}F-FDG PET	1995	USA	J Thorac Cardiovasc Surg	Yes	Yes	No	Yes	Yes	No	Yes	Yes	Yes
Naresh A. Dewan [17]	^{18}F-FDG PET	1993	USA	Chest	Yes	Yes	Yes	Yes	Yes	Yes	Yes	Yes	Yes
Naresh C. Gupta [18]	^{18}F-FDG PET	1992	USA	Radiology	Yes	No	No	Yes	Yes	Yes	Yes	Yes	Yes
Kazuo Kubota [19]	^{18}F-FDG PET	1990	Asia	J NucI Med	Yes	No	Yes	Yes	Yes	Yes	Yes	Yes	Yes
Mitsuhiro Tozaki [20]	Dynamic MRI	2005	Asia	J Comput Assist Tomogr	Yes	Yes	No	Yes	Yes	Yes	Yes	Yes	Yes
Juergen F. Schaefer [21]	Dynamic MRI	2004	Europe	Radiology	No	Yes	No	Yes	Yes	Yes	Yes	Yes	No
Yoshiharu Ohno [22]	Dynamic MRI	2002	Asia	Radiology	No	Yes	No	Yes	Yes	Yes	Yes	Yes	No
Claudius Guckel [23]	Dynamic MRI	1996	Europe	Radiology	Yes	No	Yes	Yes	Yes	Yes	Yes	Yes	Yes
Karl Hittmair [24]	Dynamic MRI	1995	Australia	Magnetic Resonance Imaging	Yes	No	Yes	Yes	Yes	Yes	Yes	Yes	Yes
Yeon Joo Jeong [25]	Dynamic CT	2005	Asia	Radiology	Yes	Yes	No	Yes	Yes	Yes	Yes	Yes	Yes
Jeong Ho Kim [26]	Dynamic CT	2004	Asia	J Comput Assist Tomogr	Yes	Yes	No	No	Yes	Yes	Yes	Yes	Yes
Jeong Ho Kim [26]	Dynamic MRI	2004	Asia	J Comput Assist Tomogr	Yes	Yes	No	No	Yes	Yes	Yes	Yes	Yes
Chin A Yi [27]	Dynamic CT	2004	Asia	Radiology	Yes	Yes	No	Yes	Yes	Yes	Yes	Yes	Yes

Table 1 (continued)

Author	Imaging modality	Year	Continent	Journal	Prodesign	Ssize30	Fulverif	Refdescr	Testdescr	Subjdescr	Report	Brdspect	Blinded
Stephen J. Swensen [28]	Dynamic CT	2000	USA	Radiology	No	Yes	No	No	Yes	Yes	Yes	Yes	No
Zhang MM [29]	Dynamic CT	1997	Asia	Radiology	No	Yes	No	Yes	Yes	Yes	Yes	Yes	No
Giuseppe Potente [30]	Dynamic CT	1997	Europe	Comput Med Imaging Graph	Yes	No	Yes	Yes	Yes	Yes	Yes	Yes	No
Stephen J. Swensen [31]	Dynamic CT	1996	USA	Radiology	No	Yes	No	Yes	Yes	Yes	Yes	Yes	No
Keiji Yamashita [32]	Dynamic CT	1995	Asia	Radiology	No	Yes	Yes	Yes	Yes	Yes	Yes	Yes	No
Stephen J. Swensen [33]	Dynamic CT	1995	USA	Radiology	No	Yes	No	No	Yes	Yes	Yes	Yes	No
Yoshiharu Ohno [34]	Dynamic CT	2019	Asia	Eur J Radiol	Yes	Yes	Yes	Yes	Yes	Yes	Yes	Yes	Yes
Yoshiharu Ohno [34]	Dynamic MRI	2019	Asia	Eur J Radiol	Yes	Yes	Yes	Yes	Yes	Yes	Yes	No	Yes
Yoshiharu Ohno [34]	^{18}F-FDG PET	2019	Asia	Eur J Radiol	Yes	Yes	Yes	Yes	Yes	Yes	Yes	No	Yes
Yoshiharu Ohno [35]	Dynamic CT	2008	Asia	J Magn Reson Imaging	Yes	Yes	No	Yes	Yes	Yes	Yes	Yes	Yes
Yoshiharu Ohno [35]	Dynamic MRI	2008	Asia	J Magn Reson Imaging	Yes	Yes	No	Yes	Yes	Yes	Yes	Yes	Yes
Yoshiharu Ohno [35]	^{18}F-FDG PET	2008	Asia	J Magn Reson Imaging	Yes	Yes	No	Yes	Yes	Yes	Yes	Yes	Yes
Yoshiharu Ohno [36]	Dynamic CT	2015	Asia	Radiology	Yes	Yes	No	Yes	Yes	Yes	Yes	Yes	Yes
Yoshiharu Ohno [36]	Dynamic MRI	2015	Asia	Radiology	Yes	Yes	No	Yes	Yes	Yes	Yes	Yes	Yes
Yoshiharu Ohno [36]	^{18}F-FDG PET	2015	Asia	Radiology	Yes	Yes	No	Yes	Yes	Yes	Yes	Yes	Yes
S W HARDERS [37]	Dynamic CT	2012	Europe	Br J Radiol	Yes	Yes	No	Yes	Yes	Yes	Yes	Yes	Yes
S W HARDERS [37]	^{99m}Tc-depreotide SPECT	2012	Europe	Br J Radiol	Yes	Yes	No	Yes	Yes	Yes	Yes	Yes	Yes
Dimitrios Boundas [38]	^{99m}Tc-depreotide SPECT	2007	Europe	Nucl Med Commun	Yes	Yes	No	Yes	Yes	Yes	Yes	No	No
Naalsund Anne [39]	^{99m}Tc-depreotide SPECT	2006	Europe	Respiration	Yes	Yes	Yes	Yes	Yes	Yes	Yes	Yes	Yes
Gibson G [40]	^{18}F-FDG PET	2017	Australia	Intern Med J	No	Yes	Yes	Yes	Yes	No	Yes	Yes	No
Suk C. Kim [41]	^{18}F-FDG PET	2008	USA	Ann Nucl Med	No	Yes	Yes	Yes	Yes	Yes	Yes	Yes	No
Nathaniel Reyes [42]	^{18}F-FDG PET	2014	USA	Lung	No	Yes	Yes	No	Yes	Yes	Yes	Yes	No
Yee Ting Sim [43]	^{18}F-FDG PET	2013	Europe	Lung	No	Yes	Yes	Yes	Yes	No	Yes	Yes	No
Stefan Walbom Harders [44]	Dynamic CT	2012	Europe	Cancer Imaging	Yes	Yes	No	No	Yes	Yes	Yes	Yes	Yes
Stefan Walbom Harders [44]	^{18}F-FDG PET	2012	Europe	Cancer Imaging	Yes	Yes	No	No	Yes	Yes	Yes	Yes	Yes
Takeshi Mori [45]	Dynamic MRI	2008	Asia	J Thorac Oncol	Yes	Yes	Yes	Yes	Yes	Yes	Yes	Yes	Yes
Takeshi Mori [45]	^{18}F-FDG PET	2008	Asia	J Thorac Oncol	Yes	Yes	Yes	Yes	Yes	Yes	Yes	Yes	Yes
Yoshiharu Ohno [46]	Dynamic CT	2013	Asia	AJR Am J Roentgenol	Yes	Yes	Yes	Yes	Yes	Yes	Yes	No	Yes
Yoshiharu Ohno [46]	^{18}F-FDG PET	2013	Asia	AJR Am J Roentgenol	Yes	Yes	Yes	Yes	Yes	Yes	Yes	No	Yes
Ye X-D [47]	Dynamic CT	2013	Asia	Clin Transl Oncol	Yes	Yes	Yes	Yes	Yes	Yes	Yes	No	Yes
Yoshiharu Ohno [48]	^{18}F-FDG PET	2017	Asia	J Magn Reson Imaging	Yes	Yes	No	No	Yes	No	Yes	No	Yes
Katsuo Usuda [49]	Dynamic MRI	2014	Asia	Asian Pac J Cancer Prev	Yes	Yes	Yes	Yes	Yes	Yes	Yes	Yes	Yes
Katsuo Usuda [49]	^{18}F-FDG PET	2014	Asia	Asian Pac J Cancer Prev	Yes	Yes	Yes	Yes	Yes	Yes	Yes	Yes	Yes
Chin A Yi [50]	Dynamic CT	2006	Asia	J Nucl Med	Yes	Yes	Yes	No	Yes	No	Yes	Yes	Yes

Table 1 (continued)

Author	Imaging modality	Year	Continent	Journal	Prodesign	Ssize30	Fulverif	Refdescr	Testdescr	Subjdescr	Report	Brdspect	Blinded
Chin A Yi [50]	^{18}F-FDG PET	2006	Asia	J Nucl Med	Yes	Yes	Yes	No	Yes	No	Yes	Yes	Yes
Jared A. Christensen [51]	Dynamic CT	2006	USA	AJR Am J Roentgenol	Yes	Yes	Yes	No	Yes	Yes	Yes	No	Yes
Jared A. Christensen [51]	^{18}F-FDG PET	2006	USA	AJR Am J Roentgenol	Yes	Yes	Yes	No	Yes	Yes	Yes	No	Yes
Yasuomi Ohba [52]	Dynamic MRI	2011	Asia	Asian Cardiovasc Thorac Ann	Yes	Yes	No	No	Yes	No	Yes	No	Yes
Yasuomi Ohba [52]	^{18}F-FDG PET	2011	Asia	Asian Cardiovasc Thorac Ann	Yes	Yes	No	No	Yes	No	Yes	No	Yes
Sun Young Jeong [53]	Dynamic CT	2008	Asia	Lung Cancer	No	Yes	Yes	Yes	Yes	Yes	Yes	Yes	Yes
Sun Young Jeong [53]	^{18}F-FDG PET	2008	Asia	Lung Cancer	No	Yes	Yes	Yes	Yes	Yes	Yes	Yes	Yes
James W. Fletcher [54]	Dynamic CT	2008	USA	J Nucl Med	Yes	Yes	No	Yes	Yes	No	Yes	Yes	Yes
James W. Fletcher [54]	^{18}F-FDG PET	2008	USA	J Nucl Med	Yes	Yes	No	Yes	Yes	No	Yes	Yes	Yes
Hung-Jen Hsieh [55]	^{18}F-FDG PET	2008	Asia	Ann Nucl Med	No	No	No	Yes	Yes	Yes	Yes	No	No
Gerarda J. Herder [56]	^{18}F-FDG PET	2004	Europe	Eur J Nucl Med Mol Imaging	No	Yes	No	Yes	Yes	Yes	Yes	No	No
Patricia Dewes [57]	Dynamic MRI	2015	Asia	Eur J Radiol	Yes	Yes	Yes	No	Yes	Yes	Yes	No	No
Paul G. Barnett [58]	^{18}F-FDG PET	2010	USA	Chest	Yes	Yes	No	Yes	Yes	Yes	Yes	Yes	Yes
Grewal RK [59]	Dynamic CT	2002	USA	Cancer J	Yes	Yes	Yes	Yes	Yes	Yes	Yes	No	Yes
Grewal RK [59]	^{99m}Tc-depreotide SPECT	2002	USA	Cancer J	Yes	Yes	Yes	Yes	Yes	Yes	Yes	No	Yes
C. J. Keith [60]	^{18}F-FDG PET	2002	Australia	Eur J Nucl Med Mol Imaging	No	Yes	No	Yes	Yes	Yes	Yes	No	No
Osamu Honda [61]	Dynamic CT	2007	Asia	J Comput Assist Tomogr	No	Yes	No	No	Yes	Yes	Yes	No	Yes
Myung Hee Chung [62]	Dynamic MRI	2000	Asia	J Magn Reson Imaging	Yes	No	No	Yes	Yes	No	Yes	No	Yes
L FAN [63]	Dynamic CT	2012	Asia	Br J Radiol	No	Yes	No	Yes	Yes	Yes	Yes	No	No
A. Maataoui [64]	Dynamic CT	2012	Europe	Pneumologie	No	Yes	Yes	Yes	Yes	Yes	Yes	Yes	No
Charles V. Zwirewich [65]	Dynamic CT	1991	USA	Radiology	No	Yes	Yes	Yes	Yes	Yes	Yes	No	No
Seemann MD [66]	Dynamic CT	1999	Europe	Eur. Radiol	Yes	Yes	Yes	Yes	Yes	Yes	Yes	Yes	Yes
YaLun Li [67]	Dynamic CT	2011	Asia	Ann Nucl Med	Yes	Yes	No	Yes	Yes	No	Yes	No	Yes
YaLun Li [67]	^{18}F-FDG PET	2011	Asia	Ann Nucl Med	Yes	Yes	No	Yes	Yes	No	Yes	No	Yes
Jarrod D. Predina [68]	^{18}F-FDG PET	2017	USA	Ann Surg	Yes	Yes	Yes	Yes	Yes	Yes	Yes	No	Yes
M.M. Schuurmans [69]	^{99m}Tc-depreotide SPECT	2007	Africa	Eur Respir J	Yes	Yes	No	Yes	Yes	Yes	Yes	No	Yes
Anna Plachci´nska [70]	^{99m}Tc-depreotide SPECT	2004	Europe	Eur J Nucl Med Mol Imaging	Yes	Yes	No	Yes	Yes	Yes	Yes	No	Yes
Andreas K. Buck [71]	^{18}F-FDG PET	2005	Europe	Eur J Nucl Med Mol Imaging	Yes	Yes	Yes	Yes	Yes	Yes	Yes	No	Yes
Steven B.Markowitz [72]	Dynamic CT	2007	USA	Chest	Yes	Yes	No	No	Yes	Yes	Yes	Yes	No
Matthew Thomas Freedman [73]	Dynamic CT	2011	USA	Radiology	No	Yes	No	No	Yes	Yes	Yes	Yes	No

Table 1 (continued)

Author	Male	Average age (year)	Number of SPN	Number of patients	tp	fp	fn	tn
Ravinder K. Grewal [1]	15	56.6	42	42	19	17	2	4
Ravinder K. Grewal [1]	15	56.6	42	42	21	12	0	9
Blum J [2]	60	64	114	114	85	7	3	19
Arnaud Halley [3]	19	59	28	28	17	3	1	7
Arnaud Halley [3]	19	59	28	28	16	2	2	8
Gerarda J. Herder [4]	15	61	36	36	13	5	1	17
Hiroaki Nomori [5]	114	61	161	161	81	21	27	32
Gang-Uei Hung [6]	14	60	26	26	19	3	1	3
Kotaro Higashi [7]	29	65	66	66	44	7	10	5
Kotaro Higashi [7]	29	65	66	66	45	7	9	5
Josephine Lee [8]	–	–	71	71	38	7	5	21
H. W. PRAUER [9]	30	59	54	54	31	11	0	12
H. W. PRAUER [9]	30	59	54	54	28	4	3	19
Val J. Lowe [10]	61	63	89	89	55	3	5	26
Naresh Gupta [11]	–	–	19	19	10	2	2	5
Robert C. Hagberg [12]	45	63	54	54	40	4	3	7
Naresh A. Dewan [13]	43	63.6	52	52	35	2	2	13
T. Bury [14]	37	64	50	50	33	2	0	15
Naresh C. Gupta [15]	45	65	61	61	42	2	3	14
Francis G. Duhaylongsod [16]	–	58	87	87	57	5	2	23
Naresh A. Dewan [17]	22	65.3	30	30	19	2	1	8
Naresh C. Gupta [18]	13	70.8	20	20	13	2	0	5
Kazuo Kubota [19]	14	–	22	22	10	1	2	9
Mitsuhiro Tozaki [20]	27	67	45	45	29	3	0	13
Juergen F. Schaefer [21]	40	61	51	51	26	3	1	21
Yoshiharu Ohno [22]	35	68	58	58	38	5	0	15
Claudius Guckel [23]	20	–	28	28	18	1	2	7
Karl Hittmair [24]	11	58	21	21	14	0	1	6
Yeon Joo Jeong [25]	62	55	107	107	46	6	3	52
Jeong Ho Kim [26]	31	–	50	50	17	10	2	21
Jeong Ho Kim [26]	38	–	54	54	21	8	0	25
Chin A Yi [27]	82	56	131	131	69	28	1	33
Stephen J. Swensen [28]	175	64.3	356	356	167	78	4	107
Zhang MM [29]	40	64	65	65	40	7	2	16
Giuseppe Potente [30]	17	60	25	25	17	2	0	6
Stephen J. Swensen [31]	57	62	107	107	51	15	1	40

Table 1 (continued)

Author	Male	Average age (year)	Number of SPN	Number of patients	tp	fp	fn	tn
Keiji Yamashita [32]	21	–	31	32	15	9	2	5
Stephen J. Swensen [33]	94	63	163	163	111	12	0	40
Yoshiharu Ohno [34]	38	69.7	71	71	46	0	7	18
Yoshiharu Ohno [34]	38	69.7	71	71	45	0	8	18
Yoshiharu Ohno [34]	38	69.7	71	71	41	3	12	15
Yoshiharu Ohno [35]	92	72.1	202	202	153	22	10	17
Yoshiharu Ohno [35]	92	72.1	202	202	157	7	6	32
Yoshiharu Ohno [35]	92	72.1	202	202	142	23	10	27
Yoshiharu Ohno [36]	111	–	218	218	148	41	17	12
Yoshiharu Ohno [36]	111	–	218	218	151	17	14	36
Yoshiharu Ohno [36]	111	–	218	218	149	38	16	15
S W HARDERS [37]	60	64	140	140	67	50	2	21
S W HARDERS [37]	60	64	140	140	65	30	4	41
Dimitrios Boundas [38]	23	62.3	57	57	22	3	1	31
Naalsund Anne [39]	77	61.7	118	118	65	15	8	30
Gibson G [40]	–	–	127	127	85	32	0	10
Suk C. Kim [41]	66	70.3	154	154	92	25	11	26
Nathaniel Reyes [42]	234	–	245	245	158	0	72	15
Yee Ting Sim [43]	77	–	186	186	138	14	20	14
Stefan Walbom Harders [44]	–	66	168	168	127	15	9	17
Stefan Walbom Harders [44]	–	66	168	168	132	17	4	15
Takeshi Mori [45]	55	70	140	140	74	1	32	33
Takeshi Mori [45]	55	70	140	140	76	7	30	27
Yoshiharu Ohno [46]	29	72.4	96	96	49	8	8	31
Yoshiharu Ohno [46]	29	72.4	96	96	36	17	21	22
Ye X-D [47]	59	59	87	87	27	12	25	23
Yoshiharu Ohno [48]	52	–	88	88	24	3	25	36
Katsuo Usuda [49]	124	68.5	189	189	128	10	32	19
Katsuo Usuda [49]	124	68.5	189	189	112	10	48	19
Chin A Yi [50]	–	–	119	119	64	3	15	37
Chin A Yi [50]	–	–	119	119	76	5	3	35
Jared A. Christensen [51]	21	66	42	42	25	12	0	5
Jared A. Christensen [51]	21	66	42	42	24	4	1	13
Yasuomi Ohba [52]	–	–	76	76	51	1	7	17
Yasuomi Ohba [52]	–	–	76	76	54	1	4	17
Sun Young Jeong [53]	56	58	100	100	33	20	7	40

Table 1 (continued)

Author	Male	Average age (year)	Number of SPN	Number of patients	tp	fp	fn	tn
Sun Young Jeong [53]	56	58	100	100	35	14	5	46
James W. Fletcher [54]	–	–	344	344	175	95	9	65
James W. Fletcher [54]	–	–	344	344	170	29	14	131
Hung-Jen Hsieh [55]	9	64	14	14	2	8	2	2
Gerarda J. Herder [56]	15	61	36	36	13	5	1	17
Patricia Dewes [57]	27	60.8	54	54	35	3	5	11
Paul G. Barnett [58]	367	65.9	375	375	194	39	10	132
Grewal RK [59]	15	56.6	42	42	19	17	2	4
Grewal RK [59]	15	56.6	42	42	21	12	0	9
C. J. Keith [60]	56	66.7	89	89	44	2	4	39
Osamu Honda [61]	45	53.7	78	78	30	7	9	32
Myung Hee Chung [62]	–	51.1	28	28	9	2	2	15
L FAN [63]	35	59.02	82	82	57	7	4	14
A. Maataoui [64]	84	63.4	129	129	89	20	5	15
Charles V. Zwirewich [65]	48	64	96	93	74	5	11	6
Seemann MD [66]	66	60.2	104	104	74	10	7	13
YaLun Li [67]	–	–	96	96	52	10	8	26
YaLun Li [67]	–	–	96	96	53	14	7	22
Jarrod D. Predina [68]	35	67	75	75	50	6	18	1
M.M. Schuurmans [69]	29	54.2	49	49	12	3	1	33
Anna Plachci´nska [70]	28	57	50	50	28	3	4	15
Andreas K. Buck [71]	31	61.9	33	33	17	4	1	11
Steven B. Markowitz [72]	–	60.6	807	807	16	27	3	761
Matthew Thomas Freedman [73]	181	60.4	368	368	80	20	42	226

CT computed tomography, *MRI* magnetic resonance imaging, ^{18}*F-FDG* fluorine 18 fluorodeoxyglucose, *PET* positron emission tomography, ^{99m}*Tc* technetium 99 m, *SPECT* single photon emission computed tomography, *SPNs* solitary pulmonary nodules, *predesign* prospective study design, *ssize30* sample size of 30 or more subjects, *fulverif* the uniform pathological biopsy reference-standard test, *refdescr* sufficient description of the reference standard, *testdescr* adequate description of the validated test, *subjdescr* sufficient clinical description of subjects, *report* adequate reporting of results, *brdspect* broad population, *blinded* blinded interpretation of test results, *tp* true-positive, *fp* false-positive, *fn* false-negative, *tn* true-negative

The details of number in the top right corner of author can be found in the supplemental data. "–" indicates not mentioned

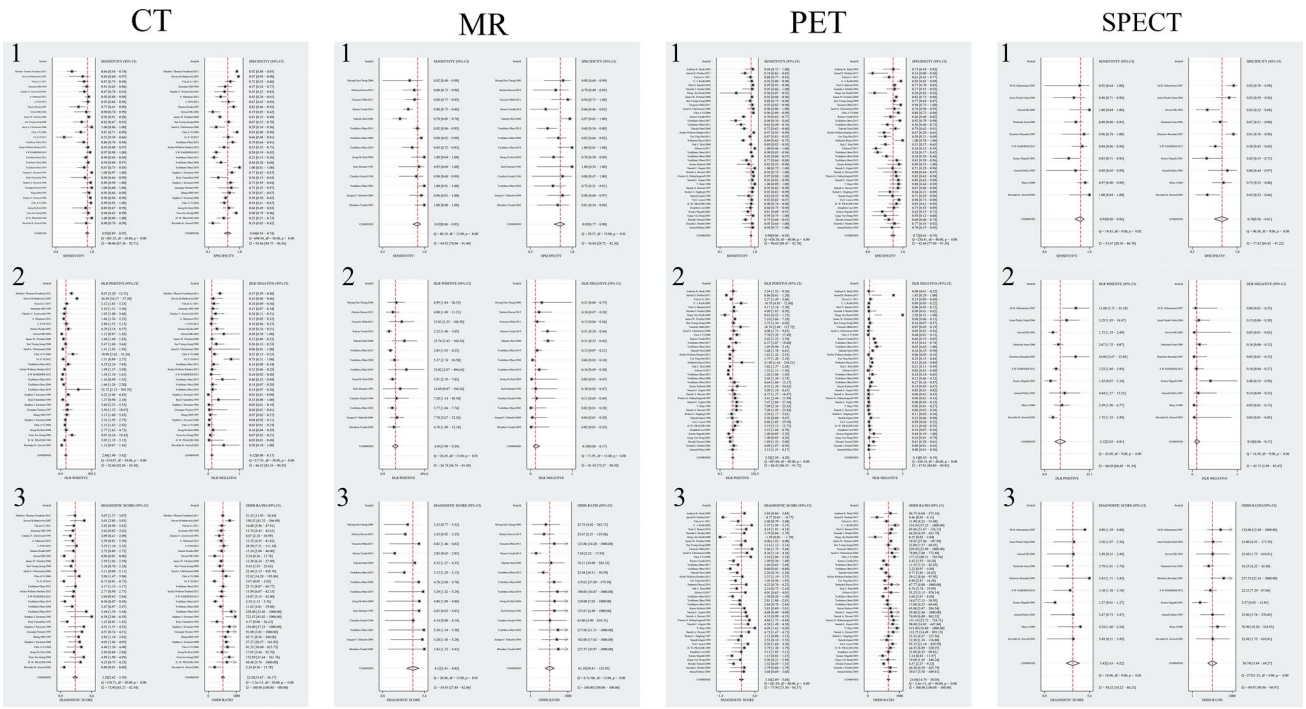

Fig. 2 The diagnostic parameters with corresponding 95% CIs for SPNs. *CT1* sensitivity and specificity of dynamic CT, *CT2* PLR and NLR of dynamic CT, *CT3* diagnostic score and DOR of dynamic CT, *MR1* sensitivity and specificity of dynamic MRI, *MR2* PLR and NLR of dynamic MRI, *MR3* diagnostic score and DOR of dynamic MRI, *PET1* sensitivity and specificity of ^{18}F-FDG PET, *PET2* PLR and NLR of ^{18}F-FDG PET, *PET3* diagnostic score and DOR of ^{18}F-FDG PET, *SPECT1* sensitivity and specificity of ^{99m}Tc-depreotide SPECT, *SPECT2* PLR and NLR of ^{99m}Tc-depreotide SPECT, *SPECT3* diagnostic score and DOR of ^{99m}Tc-depreotide SPECT

respectively. These results suggested the degree of publication bias was trivial.

Discussion

Worldwide, pulmonary cancer is ranked first malignancy. Early diagnosis and treatment play a pivotal role in yielding the favorable prognosis of the disease. Noticeably, the initial identifiable manifestation of pulmonary cancer is dominantly an SPN, whose incidence amounts to 1 per 500 images on regular chest radiographs. However, approximately half of indeterminate SPNs are confirmed as benign lesions through transbronchial/transthoracic biopsy or surgery [5–7]. Moreover, the invasive procedures are confronted with expensive cost and relevant complications and mortality [8, 9]. Hence, a non-invasive diagnostic approach for SPNs is imperative. Furthermore, a preferred technique should share the virtues of accuracy, reliability, availability, and cost-effectiveness [10]. Thereby, we compared the accuracy of the four imaging modalities for SPNs in an attempt to find an optimal non-invasive diagnostic approach.

First, the dynamic MRI has an advantage to distinguish malignant from benign SPNs, especially for pulmonary lesions with a diameter > 5 mm [11], which is characterized by non-radiation and universal applicability. In addition, when compared with other three imaging modalities, the dynamic MRI showed the well-matched diagnostic accuracy for SPNs in our study. Conventionally, the MRI was impeded to become a regular imaging fashion for SPNs due to known artifacts that result from tissue–air transitions and relatively low spatial resolution. However, several advances have been made in MRI technique (e.g., DWI [12–14], 3D GRE VIBE sequence [11, 15], ultrafast imaging techniques

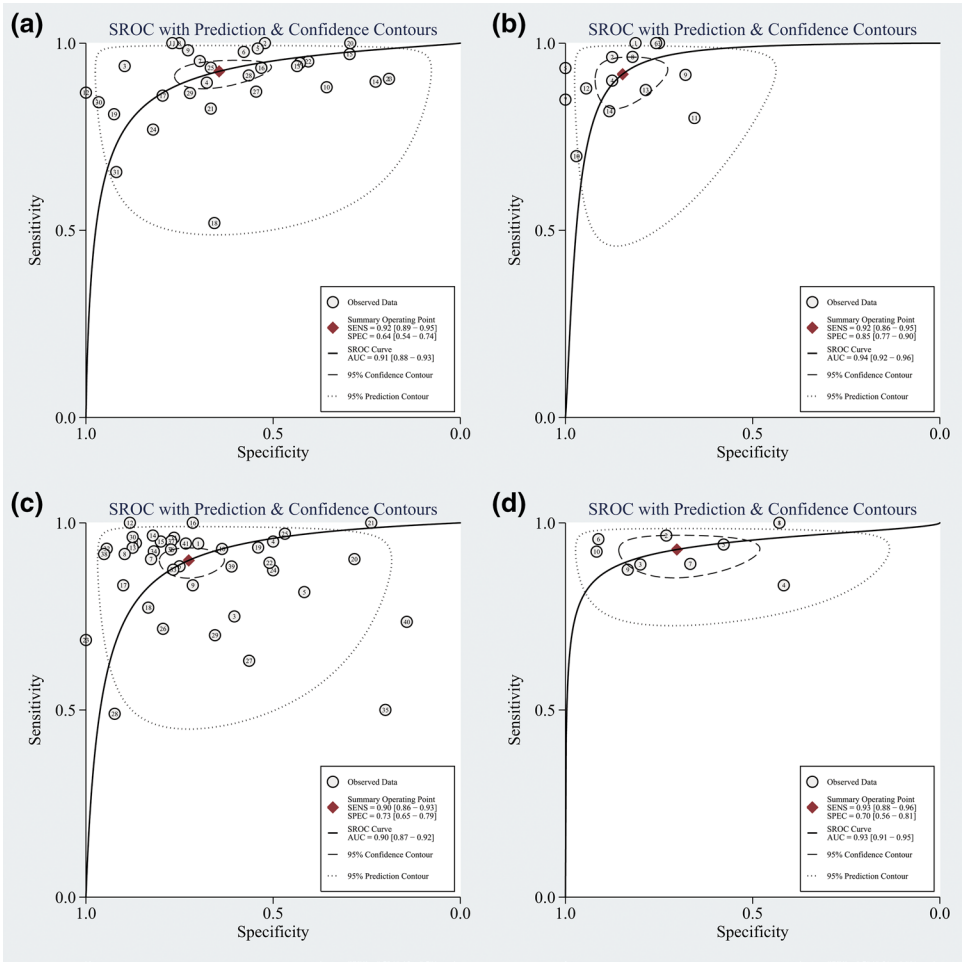

Fig. 3 Areas under SROC curves. **a** For dynamic CT; **b** for dynamic MRI; **c** for ^{18}F-FDG PET; **d** for ^{99m}Tc-depreotide SPECT

[16–18]) with the use of kinetic and morphologic parameters to improve the image quality in lung MRI and visualization of SPNs [19], which promisingly made the dynamic MRI to become an alternative standard approach for SPNs.

Secondly, the dynamic CT is distinctive in evaluating tumor vascularity and routinely applied to distinguish malignant from benign SPNs. Moreover, the recent technological advances in the form of multidetector-row CT (MDCT) contribute to accurate evaluation of hemodynamics [20–22]. Additionally, the sensitivity of dynamic CT for SPNs was further improved by combining net enhancement with washout patterns in the delayed dynamic phase. However, the fly in the ointment is that the specificity of dynamic CT is relatively low, which was also validated in our study. The reason is that some benign nodules also display enhancement in dynamic contrast-enhanced CT. Another flaw is radiation of CT. Although the application of low-dose CT for screening SPNs may reduce radiation to some degree, it comes at the cost of lower resolution.

Thirdly, ^{18}F-FDG PET, a non-invasive functional imaging, has proved to be valuable for SPNs by measuring metabolic activity via the standard uptake value (SUV) [23, 24]. Based on the U.S. bibliography, ^{18}F-FDG PET can spare unnecessary surgery in approximately 15% of individuals [25]. However, a variety of factors can impact the SUV value [26]: the body size of patient, the blood glucose concentration, the time to imaging after injection, and the nodules volume. Furthermore, this technique has defects of both high cost and radiation. Therefore, as

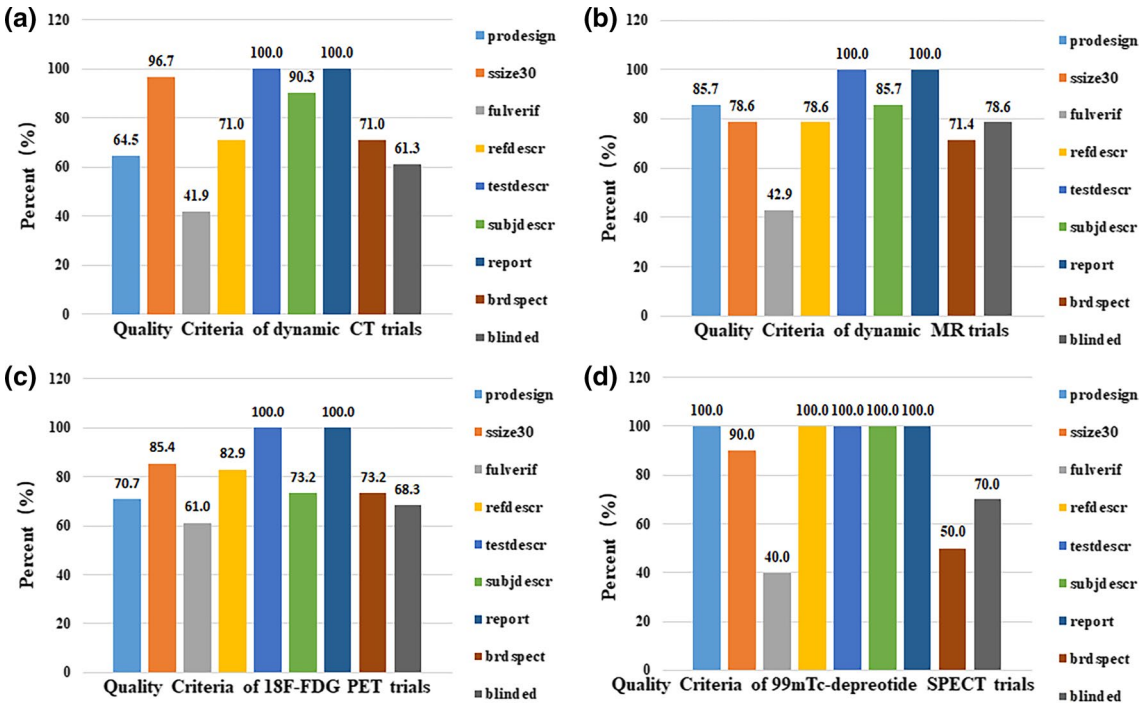

Fig. 4 Graphs illustrate the quality criteria of studies assessed in this study: **a** for dynamic CT; **b** for dynamic MRI; **c** for ^{18}F-FDG PET; **d** for ^{99m}Tc-depreotide SPECT (the percentages of trials that met the given criteria)

shown in our results, when compared with dynamic MRI and CT, the ^{18}F-FDG PET possessed no advantage in the identification of SPNs.

Finally, ^{99m}Tc-depreotide SPECT is correlated with the introduction of receptor scintigraphy and widely used in clinical practice. Based on the overexpression of somatostatin receptors on the tumor cells [27, 28], ^{99m}Tc-depreotide SPECT has been verified for the diagnosis of malignant SPNs using a ^{99m}Tc-radiolabeled somatostatin analog. From our results, the diagnostic efficacy of ^{99m}Tc-depreotide SPECT for judging SPNs resembled that of ^{18}F-FDG PET. However, it also has the disadvantage of radiation.

In summary, the dynamic MRI, dynamic CT, ^{18}F-FDG PET, and ^{99m}Tc-depreotide SPECT are all promising non-invasive approaches to distinguish malignant SPNs from benign. The dynamic MRI is the only imaging modality without radiation among the four imaging modalities. Additionally, from the viewpoint of cost-effectiveness and convenience, the dynamic MRI is superior to ^{18}F-FDG PET or ^{99m}Tc-depreotide SPECT. Thus, the dynamic MRI may serve as the preferred imaging modality for SPNs. As the development and accumulation of the medical big data, more large-scale multicenter studies for diagnosis of SPNs are recommended. Meanwhile, the artificial intelligence (AI) in imaging is emerging. An important agenda for future research for SPNs will involve image omics based on the AI and medical big data.

Limitation

This research confronted following two flaws: one was the heterogeneity among recruited trials; the other was that the information to subgroup analysis on the SPN size were unavailable.

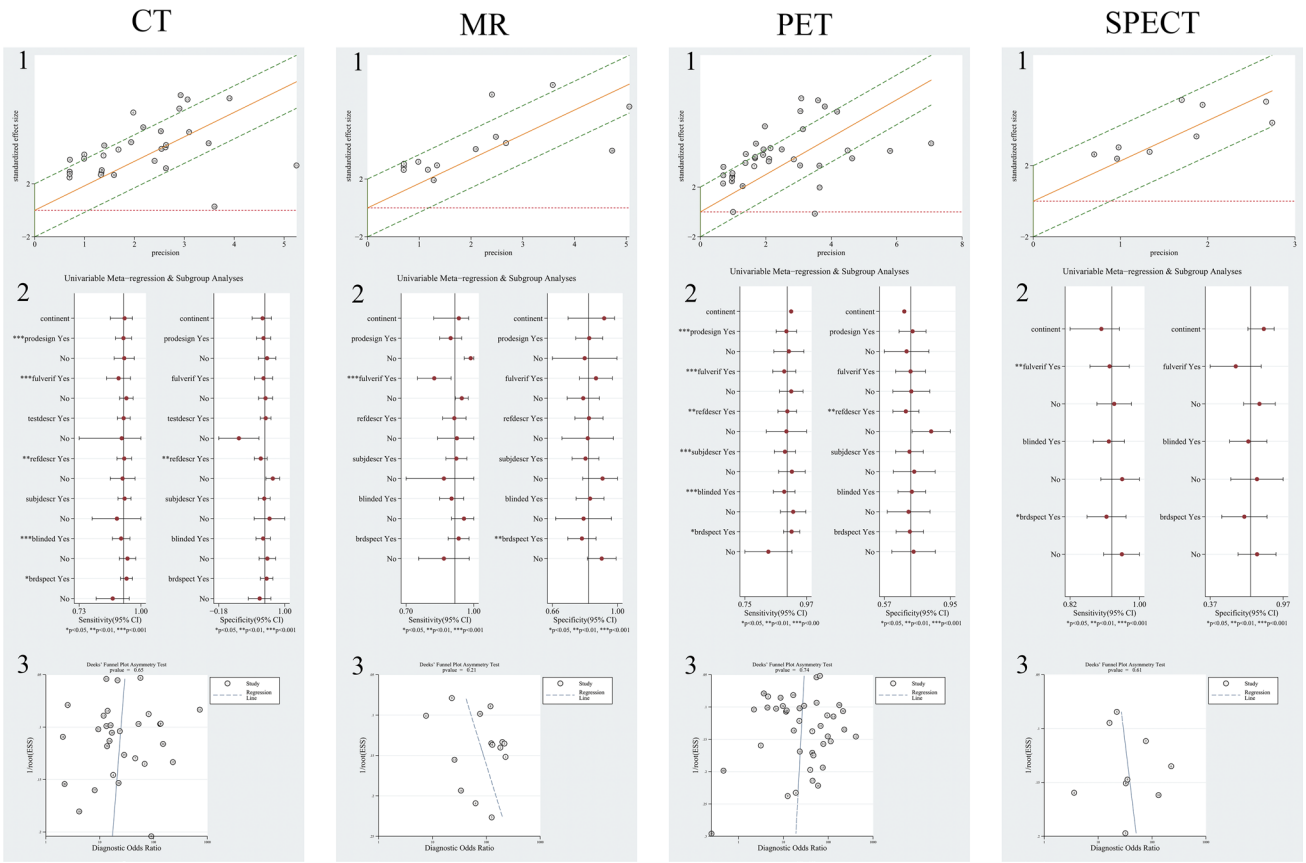

Fig. 5 The heterogeneity (Galbraith Graphs and univariable meta-regression) and asymmetry test (Deeks' Funnel Plot) of studies. *CT1* Galbraith Graph for dynamic CT, *CT2* univariable meta-regression for dynamic CT, *CT3* Deeks' Funnel Plot for dynamic CT, *MR1* Galbraith Graph for dynamic MRI, *MR2* univariable meta-regression for dynamic MRI, *MR3* Deeks' Funnel Plot for dynamic MRI, *PET1* Galbraith Graph for ^{18}F-FDG PET, *PET2* univariable meta-regression for ^{18}F-FDG PET, *PET3* Deeks' Funnel Plot for ^{18}F-FDG PET, *SPECT1* Galbraith Graph for ^{99m}Tc-depreotide SPECT, *SPECT2* univariable meta-regression for ^{99m}Tc-depreotide SPECT, *SPECT3* Deeks' Funnel Plot for ^{99m}Tc-depreotide SPECT

Conclusion

The dynamic MRI, dynamic CT, ^{18}F-FDG PET, and ^{99m}Tc-depreotide SPECT were favorable non-invasive approaches to distinguish malignant SPNs from benign. Moreover, from the viewpoint of cost-effectiveness and avoiding radiation, the dynamic MRI was recommendable for SPNs.

Acknowledgements None.

Funding None.

Compliance with ethical standards

Conflict of interest The authors declare no potential conflicts of interest.

Ethical approval This article does not contain any studies with human participants or animals performed by any of the authors.

Informed consent For this type of study, formal consent is not required.

References

1. National Comprehensive Cancer Network. NCCN Clinical Practice Guidelines in Oncology-Lung Cancer Screening (2020 Version 1). https://guide.medlive.cn/; 2020 Accessed 20 March 2020.
2. The Lung Cancer Group of Chinese Medical Association Respiratory Neurology, Chinese expert alliance of prevention and control for lung cancer. Chinese expert consensus on the diagnosis and treatment of pulmonary nodules (2018 edition). Chin Tubercul Respir J. 2018;41(10):763–771.
3. Cronin P, Dwamena BA, Kelly AM, Carlos RC. Solitary pulmonary nodules: meta-analytic comparison of cross-sectional imaging modalities for diagnosis of malignancy. Radiology. 2008;246(3):772–82.
4. Deeks JJ, Macaskill P, Irwig L. The performance of tests of publication bias and other sample size effects in systematic reviews of diagnostic test accuracy was assessed. J Clin Epidemiol. 2005;58(9):882–93.
5. Mack MJ, Hazelrigg SR, Landreneau RJ, Acuff TE. Thoracoscopy for the diagnosis of the indeterminate solitary pulmonary nodule. Ann Thorac Surg. 1993;56(4):825–30.
6. Lempel JK, Raymond DP, Usman A, Susan OM, Bolen MA, Ruffin G, et al. Video-assisted thoracic surgery resection

without intraoperative fluoroscopy after CT-guided microcoil localization of peripheral pulmonary nodules. J Vasc Interv Radiol. 2018;29(10):1423–8.
7. Keagy BA, Starek PJ, Murray GF, Battaglini JW, Lores ME, Wilcox BR. Major pulmonary resection for suspected but unconfirmed malignancy. Ann Thorac Surg. 1984;38(4):314–6.
8. Nasim F, Ost DE. Management of the solitary pulmonary nodule. Curr Opin Pulm Med. 2019;25(4):344–53.
9. Ost D, Fein AM, Feinsilver SH. Clinical practice. The solitary pulmonary nodule. N Engl J Med. 2003;348(25):2535–42.
10. Gambhir SS, Shepherd JE, Shah BD, Hart E, Hoh CK, Valk PE, et al. Analytical decision model for the cost-effective management of solitary pulmonary nodules. J Clin Oncol. 1998;16(6):2113–255.
11. Dewes P, Frellesen C, Al-Butmeh F, Albrecht MH, Scholtz JE, Metzger SC, et al. Comparative evaluation of non-contrast CAIPIRINHA-VIBE 3T-MRI and multidetector CT for detection of pulmonary nodules: in vivo evaluation of diagnostic accuracy and image quality. Eur J Radiol. 2016;85(1):193–8.
12. Usuda K, Sagawa M, Motono N, Ueno M, Tanaka M, Machida Y, et al. Diagnostic performance of diffusion weighted imaging of malignant and benign pulmonary nodules and masses: comparison with positron emission tomography. Asian Pac J Cancer Prev. 2014;15(11):4629–35.
13. Mori T, Nomori H, Ikeda K, Kawanaka K, Shiraishi S, Katahira K, et al. Diffusion-weighted magnetic resonance imaging for diagnosing malignant pulmonary nodules/masses: comparison with positron emission tomography. J Thorac Oncol. 2008;3(4):358–64.
14. Ohba Y, Nomori H, Mori T, Shiraishi K, Namimoto T, Katahira K. Diffusion-weighted magnetic resonance for pulmonary nodules: 1.5 vs. 3 Tesla. Asian Cardiovasc Thorac Ann. 2011;19(2):108–14.
15. Tozaki M, Ichiba N, Fukuda K. Dynamic magnetic resonance imaging of solitary pulmonary nodules: utility of kinetic patterns in differential diagnosis. J Comput Assist Tomogr. 2005;29(1):13–9.
16. Ohno Y, Fujisawa Y, Yui M, Takenaka D, Koyama H, Sugihara N, et al. Solitary pulmonary nodule: comparison of quantitative capability for differentiation and management among dynamic CE-perfusion MRI at 3 T system, dynamic CE-perfusion ADCT and FDG-PET/CT. Eur J Radiol. 2019;115:22–30.
17. Ohno Y, Nishio M, Koyama H, Seki S, Tsubakimoto M, Fujisawa Y, et al. Solitary pulmonary nodules: comparison of dynamic first-pass contrast-enhanced perfusion area-detector CT, dynamic first-pass contrast-enhanced MR imaging, and FDG PET/CT. Radiology. 2015;274(2):563–75.
18. Ohno Y, Koyama H, Takenaka D, Nogami M, Maniwa Y, Nishimura Y, et al. Dynamic MRI, dynamic multidetector-row computed tomography (MDCT), and coregistered 2-[fluorine-18]-fluoro-2-deoxy-D-glucose-positron emission tomography (FDG-PET)/CT: comparative study of capability for management of pulmonary nodules. J Magn Reson Imaging. 2008;27(6):1284–95.
19. Schaefer JF, Vollmar J, Schick F, Vonthein R, Seemann MD, Aebert H, et al. Solitary pulmonary nodules: dynamic contrast-enhanced MR imaging–perfusion differences in malignant and benign lesions. Radiology. 2004;232(2):544–53.
20. Ohno Y, Koyama H, Fujisawa Y, Yoshikawa T, Seki S, Sugihara N, et al. Dynamic contrast-enhanced perfusion area detector CT for non-small cell lung cancer patients: influence of mathematical models on early prediction capabilities for treatment response and recurrence after chemoradiotherapy. Eur J Radiol. 2016;85(1):176–86.
21. Ohno Y, Fujisawa Y, Koyama H, Kishida Y, Seki S, Sugihara N, et al. Dynamic contrast-enhanced perfusion area-detector CT assessed with various mathematical models: its capability for therapeutic outcome prediction for non-small cell lung cancer patients with chemoradiotherapy as compared with that of FDG-PET/CT. Eur J Radiol. 2017;86:83–91.
22. Ohno Y, Koyama H, Fujisawa Y, Yoshikawa T, Inokawa H, Sugihara N, et al. Hybrid Type iterative reconstruction method vs. filter back projection method: capability for radiation dose reduction and perfusion assessment on dynamic first-pass contrast-enhanced perfusion chest area-detector CT. Eur J Radiol. 2016;85(1):164–75.
23. Gibson G, Kumar AR, Steinke K, Bashirzadeh F, Roach R, Windsor M, et al. Risk stratification in the investigation of pulmonary nodules in a high-risk cohort: positron emission tomography/computed tomography outperforms clinical risk prediction algorithms. Intern Med J. 2017;47(12):1385–92.
24. Predina JD, Newton AD, Keating J, Barbosa EM Jr, Okusanya O, Xia L, et al. Intraoperative molecular imaging combined with positron emission tomography improves surgical management of peripheral malignant pulmonary nodules. Ann Surg. 2017;266(3):479–88.
25. Lillington GA, Gould MK. Managing solitary pulmonary nodules: accurate predictions and divergent conclusions. Mayo Clin Proc. 1999;74(4):435–6.
26. Nomori H, Watanabe K, Ohtsuka T, Naruke T, Suemasu K, Uno K. Visual and semiquantitative analyses for F-18 fluorodeoxyglucose PET scanning in pulmonary nodules 1 cm to 3 cm in size. Ann Thorac Surg. 2005;79(3):984–8.
27. Raslan OA, Parkar ND, Muzaffar R, Doherty C, Osman MM. Case 227: endobronchial carcinoid tumor with incidental metastatic breast cancer detected with somatostatin receptor scintigraphy ((111) in pentreotide). Radiology. 2016;278(3):949–55.
28. Krenning EP, Kwekkeboom DJ, Bakker WH, Breeman WA, Kooij PP, Oei HY, et al. Somatostatin receptor scintigraphy with [111In-DTPA-d-Phe1]-and [123I-Tyr3]-octreotide: the Rotterdam experience with more than 1000 patients. Eur J Nucl Med. 1993;20(8):716–31.